OPTO-ELECTRONICS REVIEW 8(4), 421–425 (2000)

X-ray diffracting investigation of strain distribution in silicon implanted by phosphorus

Z. ŚWIĄTEK[1], J. BONARSKI[1], R. CIACH[1], I.M. FODCHUK[2*] M.D. RARANSKY[2], and O.G. GIMCHINSKY[2]

[1]Institute of Metallurgy and Material Science, Polish Academy of Sciences
25 Reymonta Str., 30-059 Cracow, Poland
[2]Chernivtsi State University, 2 Kotsyubynsky Str., 58012 Chernivtsi, Ukraine

Research of structural changes in subsurface layers of Si single crystals during formation of amorphous layers hidden under the surface are carried out. It is established that phosphorus ion (with 180 keV energy and a doze of the order of 10^{15} ion/cm^2) implantation and subsequent short-term temperature annealing at T = 500°C are caused great structural changes in subsurface areas. The great strains in direction perpendicular to interface are characteristic of structures formed in this way.

Keywords: X-ray diffracting, subsurface layers, Si single crystals.

1. Introduction

Radiating defects arise at interaction of ions accelerated and crystals, as well as phenomena of internal ionisation and implantation of foreign atoms in crystal. The nuclear collisions are accompanied by the large losses of energy of ion and changed direction of its motion. This lead to the distortion of target structure and creation on the track of implantation ion the depletion layers-clusters. Clusters are areas with the high concentration of point defects. The sizes of clusters can reach 10 nm and more. Clusters merged at large stream density of implanted ions and created continuous layer. Then relative state structure defects are arisen as result of interaction of primary point defects to one another and with impurities. At the same time dislocation loops are appeared in wedges of displacement or areas of impulse overheating near stopping implanted ion. These combined effects have strong influence on the properties of irradiated materials [1].

It is possible now to select conditions of ionic implantation and annealing defects so that the significant part of the interstitial atoms of impurity becomes electrically active [2,3]. For photogalvanic conversion of spectrum energy the amorphous silicon in infrared region of solar spectrum has greater absorption coefficient ($\beta \geq 10^2$ cm^{-1}) than monocrystalline silicon. However, it has considerably worse electronic properties. The new, perspective solution of rising efficiency of conversion of solar spectrum energy is seen at overlapping of amorphous and crystalline phases in one optoelectronic device [3].

2. Research results

This work represent X-ray investigation of strains, that arise in transition layers of division boundaries at the creation so-called δ-BSF structure (δ is the thin implanted layer) by ionic implantation of phosphorus ions in monocrystalline silicon. The researches were carried out for four groups of silicon samples [diameter is 50 mm, width 250 μm, entry surface (001)], which distinguished by the form of a hidden substructure. Only half of surface square in a sample was influenced by radiation for convenience of the analysis. Temperature of annealing is 500°C. Annealing time for a sample No. 2 is 6 minutes, No. 3 is 15 minutes and No. 4 is 30 minutes. Implantation was carried out to eliminate the canal effect. Energy of implantation ions was E = 180 keV, doze ~10^{15} ion/cm^2. At these dozes and energies of implantation the crystalline structure is disturbed with creation of the numerous disordered areas, where considerable density of point defects is concentrated and lead to the changes of optical surface properties of silicon layers. According to the data obtained from electron microscopy with high resolution the formed transition layers consist of hollows and rises that cause two-dimensional and three-dimensional distortions [2].

It is very important to have enough detailed information about a set of emerging defects and amorphism degree immediately after ionic implantation at room temperature and after annealing. Therefore, we used a combine of different X-ray methods for detection of the strains emerging in volume and structural changes in surface layer of silicon after implantation and following annealing. One and two-crystalline schemes (n, –n) are used for the layerwise analysis of structural changes in surface layers [4]. Researched crys-

* e-mail: ifodchuk@phys.chsu.cv.ua

tal is installed in symmetric and skew-asymmetric diffraction scheme on reflection. Symmetric (400) $CuK_{\alpha 1}$ and "skew- -asymmetric" (331) CoK_{α} reflections are chosen for the investigation. In the second case the angles of the diffraction θ and disorientation Ψ (between entry (001) and reflecting planes) insignificantly differ ($\theta - \Psi \approx 1°$). The angles of inputting and outputting of X-rays at the azimuth turn of crystal around diffraction vector at the angle in skew- -asymmetric scheme of the diffraction vary as follows [5]

$$\sin(\Phi_{0,h}) = \gamma_{0,h} = \pm\sin(\theta)\cos(\psi) - \cos(\theta)\sin(\psi)\cos(\varphi). \quad (1)$$

The sign "+" concerns an incident ray and sign "–" diffracted one. It follows from Eq. (1), that for crystal turns at the angle φ, the smooth conversion from Laue diffraction to the Bragg diffraction is ensured. It should be noted, that contrary to usual geometry of diffraction, in skew-asymmetric scheme it is possible to select the cases, by changing the angle φ, when the layers studied after implantation have the location depth less than extinction depth $\Lambda = \left(\lambda/|\chi_h|\right)\left(\gamma_0/\gamma_h\right)^{1/2}$, ($\chi_h$ is the Fourier coefficients of polarisability, λ is the wavelength).

Initial crystal was used as the standard for obtaining real picture about deforming processes in samples. The obtained results (Figs. 1–4) demonstrate structural changes in surface layers of the irradiated crystals, which are accompanied by formation active heteroboundary. It involves considerable strains in crystal surface layer. These strains are caused by creation of thermodynamic nonequilibrum structural defects of various types during ionic implantation [1–4]. The probability of defect formation is increased at given energy and ion doze in the following sequence: atoms in interstitial sites, vacancies, Ffenkel pairs, complexes and accumulations of vacancies and interstitial atoms, dislocation loop, disordered areas, amorphous areas.

The qualitative topographical results (Fig. 1) supplemented quantitative ones, obtained from dependencies of rocking curves (Fig. 2). The method of the integrating characteristics is used also for investigation of initial samples. Survey of the profile of intensity distribution for the reflected beam $I_R(x)$ on the base of Borman fan (Fig. 3), at the diffraction $MoK_{\alpha 1}$- and MoK_{β}- radiation, was carried out by turning of the detector arrow with the narrow entry window (0.05 mm) on the small angles $\Delta\varphi$ in the range of Bragg angle (Fig. 3). The profiles $I_R(x)$ are measured for reflexes with different order for the planes (400) and (800). The divergence of a primary beam was 5′ approximately.

The analysis of data obtained from non-irradiated and irradiated half of plate give the following picture. Since a crystal depth of the order Λ = 1 μm in the irradiated half a half-width of rocking curve is gradually increased (on the average of 15–20%, and at Λ ~0,5 μm the X-ray diffracting reflection is completely neutralised. On the "tails" of the rocking curve, significant diffuse scattering is appeared. Integrated reflectivity of a crystal is increased. The value of

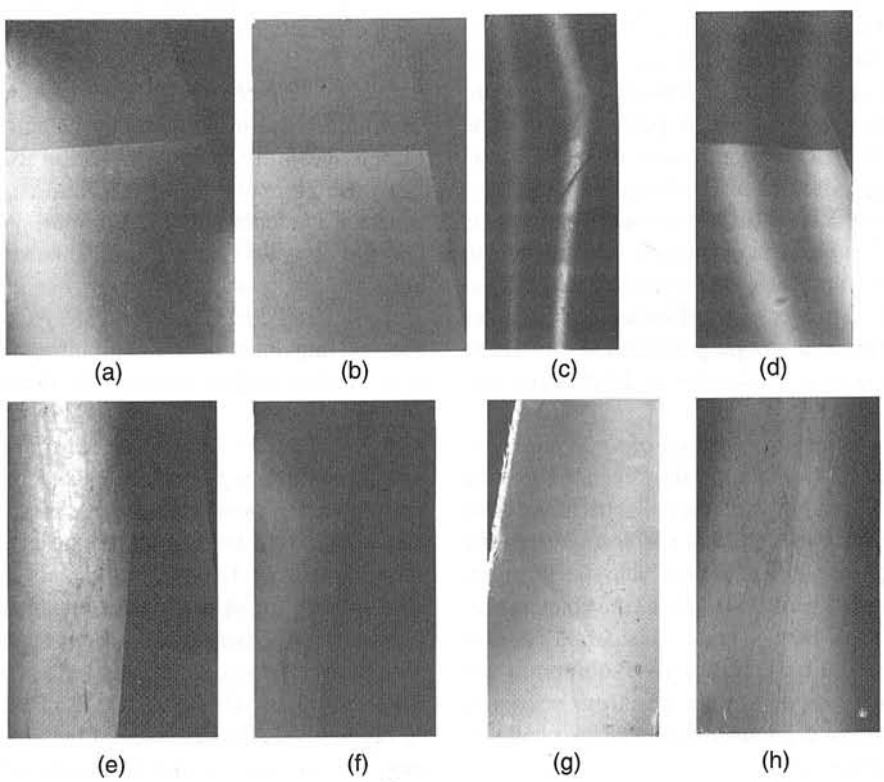

Fig. 1. X-ray topographs obtained on skew-asymmetric diffraction scheme for (331) reflection of CoK_{α}. Entry surface is (001). Before annealing [(a) and (b)], after annealing [(c), (d), (e), (f), (g), and (h)]. Λ = 0.74 μm (a), Λ = 0.5 μm (b), Λ = 0.65 μm (c), Λ = 0.44 μm (d). Sample No. 2 [(c) and (d)], sample No. 3 [(e) and (f)], sample No. 4 [(g) and (h)].

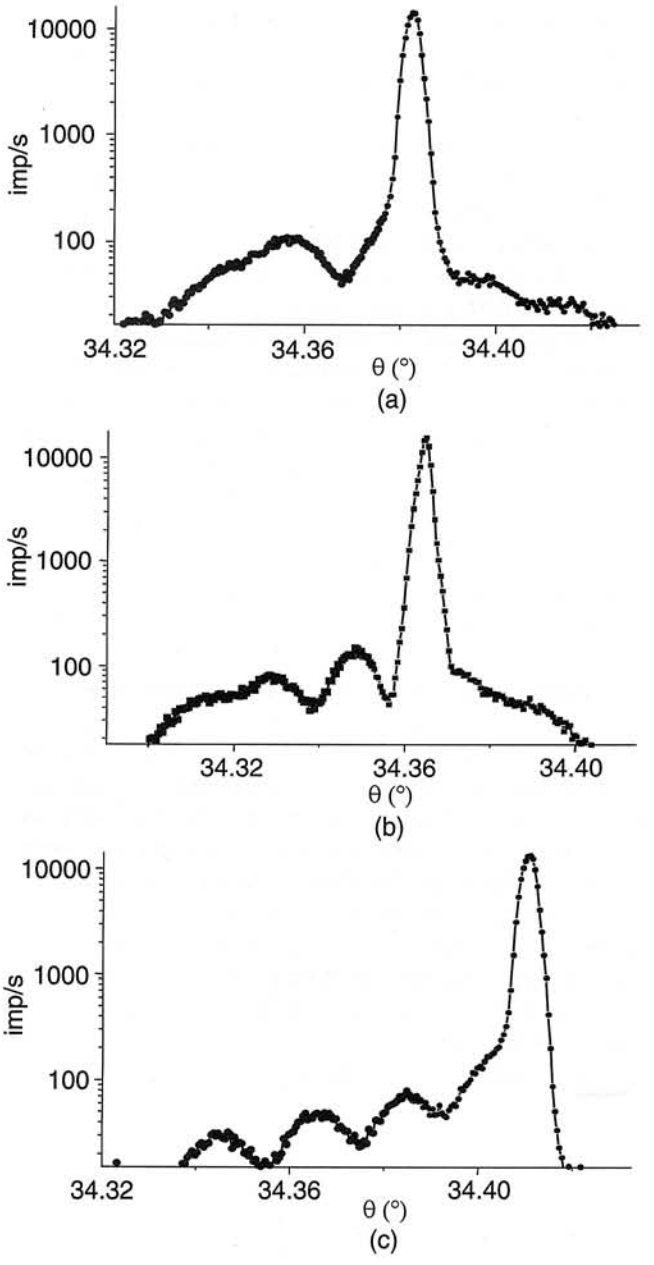

Fig. 2. Rocking curves obtained at symmetric reflection (400) of CuKa for samples: No. 1(a), No. 2(b), No. 4(c). Scheme (n, –n).

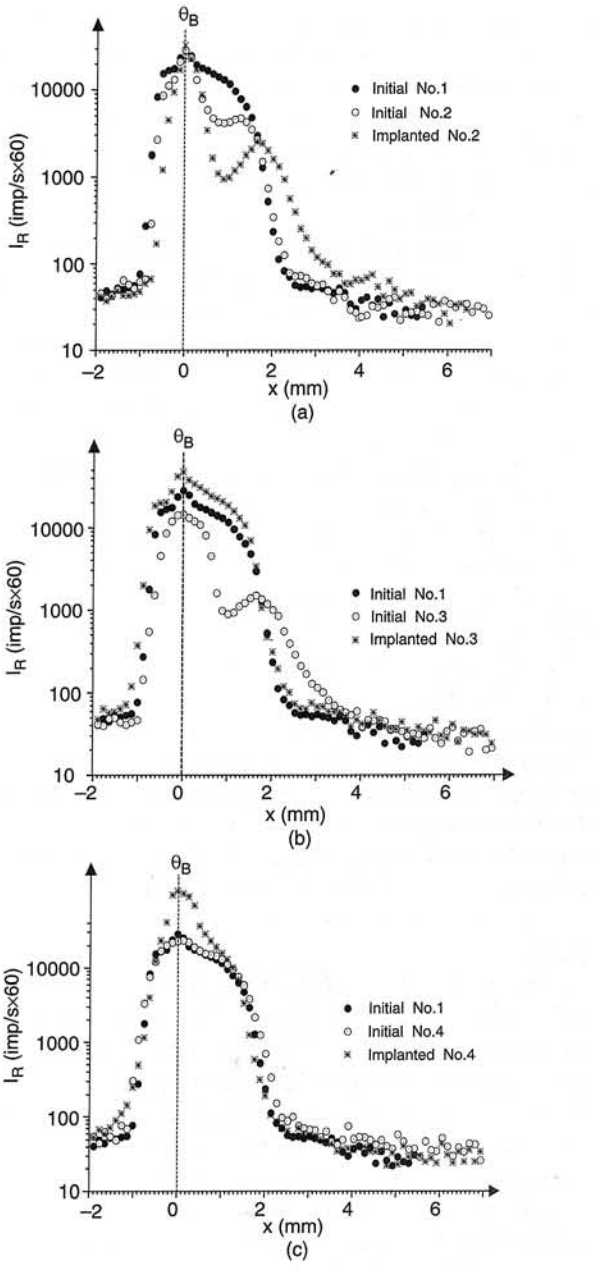

Fig. 3. Profiles of space distributions of integrating intensity after annealing: t_0 = 6 minutes (a), t_0 = 15 minutes (b), t_0 = 30 minutes (c).

maximum intensity of reflection in exact diffraction position is decreased on the average of 10–15%. Such behaviour of the called parameters of structural perfection indicated about an origin of strain fields in surface layer both local and extended, that is a consequence of damaging surface layers during ionic implantation.

The method founded on Fourier analysis is used to the quantitative analysis of the rocking curves [4]. It had allowed calculate the effective width of damaged layer L_{ef}, the value of average deformation of a crystalline lattice $\bar{\varepsilon} = (\Delta d/d)$ and value of root-mean-square deformation. The effective localisation depth of large damages is within 0.4 to 0.5 μm at the implantation method of creating amorphous layers hidden under surface. This depth exceeds nearly in two times the length of free run for phosphorus ions at such energies and dozes. The area of elastic deformations is extended to depth of 1.1–1.2 μm. The maximum strain value in transition layer is ~3.6×10^{-3}. Radiating defects in transition area under amorphous layer predetermine appearance of positive lattice deformations in it with the value of ε ~$(3–5)\times10^{-4}$. The thickness of layer reached ~0.3 μm, and thickness of transition layer between amorphous area and crystal was ~0.2–0.4 μm. The value of the Debye-Waller factor L for (400) and (800) reflections of MoK_α varies within 5.4×10^{-2} to 1.1×10^{-1}, parameter of the diffuse losses μ_d – from 2.8 to 5.7 cm^{-1}. It is equivalent to availability of

cluster derivations with sizes of the order R = 10^{-6} cm at the concentration of dislocation loops C_L ~10^{12}–10^{13} cm^{-2}.

After ionic bombardment crystal surface layers are in structurally metastable state. Postimplantation annealing was carried out to the transition of phosphorus impurity in more stable position at T = 500°C.

X-ray diffraction investigations of annealing time influence on division boundary surface-implantation layer-matrix are evidence of the following. The structural relaxation in the layer hidden under surface caused mesoscopic heterogeneity of strain distribution, and as the result to the local increasing of internal strains. The essential difference in strain distribution normally and in parallel way to heteroboundary is observed.

According data of high resolving electron microscopy at short-term temperature anneal (the sample No. 2) the considerable "clusterisation" of the surface and incomplete recrystallisation of damaged layers are observed. It is mapped on the strain distribution in crystal depth that it is formatted from reflection curves. In the direction perpendicular to the boundary the strain value varies from $\varepsilon \approx 3.1\times10^{-3}$ at the annealing time t_o = 6 minutes to $\varepsilon \approx 6\times10^{-3}$ at t_o = 30 minutes. The value of the Debye-Waller factor L increases from 1.67×10^{-2} to 4.6×10^{-2} for reflection (400) MoK_α. The tendency of increasing dislocation loop size and decrease it density at increasing of anneal time is observed: at t_o = 6 minutes – $C_L = 1.5\times10^{11}$ cm^{-2}, R = 20 nm and at t_o = 30 minutes – $C_L = 1.5\times10^{10}$ cm^{-2}, R = 50 nm.

Increase in anneal duration (sample No. 3) caused more intensive recrystallisation of amorphous layer, that identified by profiles of deformations. Width of transition crystalline area increased to 0.1–0.15 μm. Average relative deformation value is 10^{-4}. Negative strains of the crystalline lattice appeared that could be caused by substitution Si in lattice sites by phosphorus atoms with smaller tetrahedral covalent radius, as well as by great defection of recrystallised layer. The increase of annealing time carries to growth of layer width and strain value of both signs. Let's remark that widening reflection curves reduce calculation accuracy of the integrated characteristics. At that the deformation of tensile can be influenced by dislocation loops of interstitial type [10]. Such deformations are caused also by lattice compression due to precipitating of selections of various sorts, for example SiC. The average value of estimated negative strains is significant less than real.

At the longer annealing (sample No. 4), as well as in the previous cases – decrease in strains in transition layers are not observed, that means transformation of amorphous phase in polycrystalline and a large deformation of boundary. The large density of various microdefects with different size is contained in structure obtained by this method. It is observed on the curve of diffraction reflection as additional maxima outside of angle area that corresponded to reflection maxima for substrate.

It is necessary to pay attention on significant influence of elastic strains on formatting of X-ray reflection curves and space intensity distributions. Such influence can be explained at assuming that the process of defect modification is not atomic, but collective, i.e., large number of elementary defects and crystal atoms are take part in process synchronously. This process of structural modification is expanding to the large distances from boundary 1.1–1.3 μm. Indeed, we can stimulate decay of small-sized clusters with consequent coagulation of point defects in larger clusters if the continuance of the annealing process of the cluster is longer than the time of deforming stretch to the transformation of each defect within cluster [3].

The static elastic strains can influenced in essential manner on the rate of the structural defect modification in silicon. Its role appears during formation of residual defecting implantation layer during it irradiation in places of space discontinuity of mechanical strains in crystal. In these areas diffraction reflexes also are smeared and more distorted on topographs, the half-width of the rocking curves increased, the transformation of the space form of intensity distributions and considerable growth of diffuse background is observed (Fig. 3).

3. Simulating profiles of strain distribution

On the basis developed technique within kinematics theory of X-ray scattering the computer simulations of strain distributions are carried out for crystal after ionic implantation. On the given distribution of deformations rocking curve of X-ray is calculated and compared with experimental rocking curve [8]. By means of functional definition of strain and deviation profile and optimisation of their parameters the computer modelling of theoretical rocking curves was carried out to obtaining their satisfactory coincidence with experimental.

The distribution of elastic deformation $\Delta d(z)/d$ and distortions W(z) is as follows

$$\frac{\Delta d(z)}{d} = \begin{cases} x_2 \exp\left[-\left(\dfrac{z-x_1}{2x_3}\right)^2\right], & \dfrac{\Delta d}{d} > x_5, \text{ and } z \le x_1 \\ x_5, & \dfrac{\Delta d}{d} \le x_5 \text{ and } z \le x_1 \\ x_2 \exp\left[-\left(\dfrac{z-x_1}{2x_4}\right)\right]^2, & z > x_1 \end{cases} \quad (2)$$

$$W(z) = \begin{cases} x_7 \exp\left[-\left(\dfrac{z-x_1}{2x_4}\right)^2\right], & z > x_{10} \\ x_{10}, & W \le x_{10} \text{ and } z \le x_6 \\ x_7 \exp\left[-\left(\dfrac{z-x_6}{2x_3}\right)^2\right], & z > x_6 \end{cases} \quad (3)$$

All the parameters in Eqs. (2) and (3), except x_2, x_5, x_7, x_{10}, are assigned through the extinction length Λ. It should

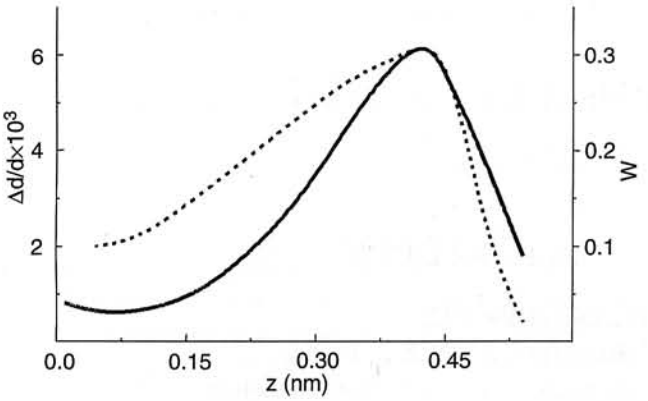

Fig. 4. Reproduced profiles of deformations (dotted line) and distortions (solid line).

be noted, that in skew-asymmetric scheme of diffraction contrary to usual one, extinction length can vary smoothly more than on two order, i.e., it can considerably exceed or to be commensurable with effective length of strain change in surface layers [5–8].

The experimental rocking curves are obtained on double-crystalline x-ray spectrometer in skew-asymmetric scheme of diffraction with using (331) CoK_α radiation. As a whole, the reproduced profile of deformations and distortions (Fig. 4) in Si, implanted by P^+ ions, is not symmetrical. Thus, the combined using of topographical and diffractometer methods permit determining structural changes and strain distributions, which arisen in surface layers of monocrystalline silicon at formatting hidden boundaries by ionic implantation.

References

1. H. Rassel and Ruge, *Ionic Implantation*, Nauka, Moscow, 1983.
2. Z.T. Kuznicki, "L-H interface improvement for ultra high efficiency Si solar cells," *J..Appl. Phys.* **74**, 2058–2063 (1993).
3. Z.T. Kuznicki, "Betterment of infrared characteristics of monocrystalline silicon at implantation," *Neorganicheskie Materialy* **33**, 142–146 (1997).
4. S.A. Kshevetsky, Yu.P. Stetsko, I.M. Fodchuk, I.V. Melnychuk, and V.S. Polyanko, "Skew-asymmetric X-ray topography of surface layers in monocrystals," *Ukrainian J. Physics* **30**, 344–348 (1990).
5. A.M. Afanasiev, P.A. Aleksandrov, and R.M. Imamov, *X-ray Diffraction of Submicron Layers*, Nauka, Moscow, 1989.
6. S.A. Stepanov, E.A. Kondrashkina, and A.H. Chuzo, "The more refined method of integral characteristics for X-ray diffraction analysis of surface layers in monocrystals," *Poverkhnost* **9**, 112–118 (1988).
7. V.G. Kohn, M.V. Prilepsky, and I.M. Suhodreva, "Simple method of determining structure of distorting surface layers in monocrystals from X-ray diffraction data," *Poverkhnost* **4**, 122–127 (1984).
8. R.N. Kyutt, P.V. Petrachen, and L.M. Sorokin, "Strain profiles in ion-doped silicon obtained from X-ray rocking curves," *Phys. Stat. Sol. (a)* **50**, 381–389 (1980).
9. A.L. Golovin, R.M. Imamov, and E.A. Kondrashkina, "Potentialities of new X-ray diffraction methods in structural studies of ion-implanted silicon layers," *Phys. Status Solidi (a)* **88**, 505–514 (1985).
10. M. Servidori, "Characterisation of lattice damage in ion implanted silicon by multiple crystal X-ray diffraction," *Nuclear Instruments and Methods in Physics Research* **19/20**, 443–449 (1987).
11. B.C. Larson and J.F. Barhorst, "X-ray study of lattice strain in boron implanted laser annealed silicon," *J. Appl. Phys.* **51**, 3181–3185 (1980).